Science of the Total Environment 759 (2021) 143486

Contents lists available at ScienceDirect

Science of the Total Environment

journal homepage: www.elsevier.com/locate/scitotenv

The influence of summer hypoxia on sedimentary phosphorus biogeochemistry in a coastal scallop farming area, North Yellow Sea

Bo Yang [a,b,c], Xuelu Gao [a,b,c,*], Jianmin Zhao [a,c], Yongliang Liu [a,b], Tianci Gao [a,b], Hon-Kit Lui [d], Ting-Hsuan Huang [d], Chen-Tung Arthur Chen [d], Qianguo Xing [a,c]

[a] CAS Key Laboratory of Coastal Zone Environmental Processes and Ecological Remediation, Yantai Institute of Coastal Zone Research, Chinese Academy of Sciences, Yantai, Shandong 264003, China
[b] University of Chinese Academy of Sciences, Beijing 100049, China
[c] Center for Ocean Mega-Science, Chinese Academy of Sciences, Qingdao, Shandong 266071, China
[d] Department of Oceanography, National Sun Yat-sen University, Kaohsiung 80424, Taiwan

HIGHLIGHTS

- Sedimentary P cycle was largely affected by summer hypoxia and scallop farming.
- The benthic P flux was mainly controlled by the remobilizing of Fe—P, OP and Ex-P.
- In August, ~0.92 μmol g^{-1} of Fe—P was converted into DIP and released into water.
- ~0.52 and ~0.54 μmol g^{-1} of OP was transformed into DIP in August and November.
- ~0.36 and ~0.55 μmol g^{-1} of DIP was adsorbed to clay minerals in the two months.

GRAPHICAL ABSTRACT

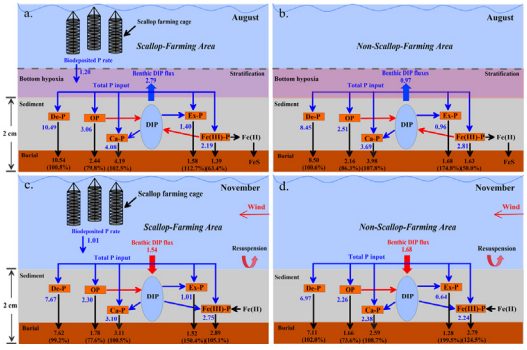

ARTICLE INFO

Article history:
Received 28 July 2020
Received in revised form 22 October 2020
Accepted 25 October 2020
Available online 11 November 2020

Dr. Julian Blasco

Keywords:
Mariculture area
Coastal environment
Laboratory incubation
Phosphorus fractionation
Sediment analysis
Sequential extraction

ABSTRACT

In situ field investigations coupled with laboratory incubations were employed to explore the surface sedimentary phosphorus (P) cycle in a mariculture area adjacent to the Yangma Island suffering from summer hypoxia in the North Yellow Sea. Five forms of P were fractionated, namely exchangeable P (Ex-P), iron-bound P (Fe—P), authigenic apatite (Ca—P), detrital P (De-P) and organic P (OP). Total P (TP) varied from 13.42 to 23.88 μmol g^{-1} with the main form of inorganic P (IP). The benthic phosphate (DIP) fluxes were calculated based on incubation experiments. The results show that the sediment was an important source of P in summer with ~39% of the bioavailable P (Bio—P) recycled back into the water column. However, the sediment acted a sink of P in autumn. The benthic DIP fluxes were mainly controlled by the remobilizing of Fe—P, Ex-P and OP under contrasting redox conditions. In August (hypoxia season), ~0.92 μmol g^{-1} of Fe—P and ~0.52 μmol g^{-1} of OP could be transformed to DIP and released into water, while ~0.36 μmol g^{-1} of DIP was adsorbed to clay minerals. In November (non-hypoxia season), however, ~0.54 μmol g^{-1} of OP was converted into DIP, while ~0.55 μmol g^{-1} and ~0.28 μmol g^{-1} of DIP was adsorbed to clay minerals and bind to iron oxides. Furthermore, scallop farming activities also affected the P mobilization through biological deposition and reduced hydrodynamic conditions. The burial fluxes of P varied from 11.67 to 20.78 μmol cm^{-2} yr^{-1} and its burial

* Corresponding author at: CAS Key Laboratory of Coastal Zone Environmental Processes and Ecological Remediation, Yantai Institute of Coastal Zone Research, Chinese Academy of Sciences, Yantai, Shandong 264003, China.
E-mail address: xlgao@yic.ac.cn (X. Gao).

https://doi.org/10.1016/j.scitotenv.2020.143486

efficiency was 84.7–100%, which was consistent with that in most of the marginal seas worldwide. This study reveals that hypoxia and scallop farming activities can significantly promote sedimentary P mobility, thereby causing high benthic DIP flux in coastal waters.

1. Introduction

Phosphorus (P), an indispensable nutrient in aquatic environment, plays a significant role in regulating biological community structure and biogeochemical cycle of biogenic elements (Kang et al., 2017; Liu et al., 2016, 2019). For example, excess loading of active P into waters can adversely affect the aquatic system, e.g. water eutrophication, harmful algal blooms and hypoxia (Adhikari et al., 2015; Lin et al., 2016; Rucinski et al., 2016).

The P in water is mainly originated from external input, e.g. atmospheric deposition, river input and groundwater discharge, and sediment release (Yang et al., 2017). In coastal waters significantly affected by human activities, e.g. aquaculture activities, sediment has a more important influence on P cycle due to high biodeposition rate, which may act both as a source and a sink of P in water (Zhang et al., 2013a; Pan et al., 2020).

Generally, the remobilizing of P at the sediment-water interface is mainly controlled by the geochemical characteristics of different sedimentary P forms (Mort et al., 2010; Liu et al., 2020). Exchangeable P (Ex-P), iron-bound P (Fe—P), authigenic apatite P (Ca—P), detrital P (De-P) and organic P (OP) are widely recognized as the main forms of sedimentary P (Ruttenberg, 1992). Different P fractions have different geochemical behaviors, and only certain forms of P, i.e. Ex-P, Fe—P and OP, can be transformed into bioavailable ones and released into the water column under various physico-chemical processes, e.g. dissolution, desorption and reduction (Song, 2010).

Many environmental factors, such as grain-size of sediment, redox characteristics, temperature and pH, can all affect the geochemical process (e.g. preservation, transformation and recycling) of sedimentary P (Liu et al., 2016, 2020; Pan et al., 2020). It is widely believed that dissolved oxygen (DO) is one of the most important parameters controlling the P cycle in aquatic ecosystems, which is mainly driven by the Fe—P migration in sediments (Liu et al., 2020). Generally, oxygen-rich sediments are favorable for the formation of Fe—P. In contrast, large amounts of P can be released back into the water due to reductive dissolution of Fe/Mn oxides under hypoxic conditions. Moreover, hypoxic environments can facilitate the anaerobic decomposition of organic matter (OM) to a certain extent, thereby accelerating the P cycle (Picard et al., 2019).

Mariculture activities, especially shellfish farming, can also affect the P cycle in coastal waters (Liu et al., 2016a). This occurs because shellfish usually feed on phytoplankton and then repackage them into rapidly settling biodeposits, i.e. faeces and pseudofaeces, which accelerates the accumulation of OP in the sediment. Furthermore, the increased sediment organic matter (SOM) can promote the DO consumption, thereby creating a hypoxic environment, which accelerates the turnover and redistribution of P in the ecosystem (Zhao et al., 2019).

The coastal waters around the Yangma Island, as an important scallop farming zone, are located in the North Yellow Sea (NYS) next to the north coastline of the Shandong Peninsula. Scallop farming activities have been found significantly increasing the content of OM in this area (Zhang et al., 2018; Yang and Gao, 2019). In summer, the combination of high OM productivity, high temperature and low wind speed induces the rapid depletion of DO and subsequent hypoxia, which have greatly affected the biogeochemical cycle of biogenic elements (Yang et al., 2018; Yang and Gao, 2019). However, sedimentary P cycling processes and its release mechanisms in this area remains unknown. Thus, this study investigated the biogeochemical cycling process of P in sediments of coastal waters around the Yangma Island via a series of in situ field investigations coupled with laboratory incubations with the following objectives: (1) to identify the seasonal variations of sedimentary P species and their influencing factors, and (2) to clarify the sedimentary P burial and release mechanisms.

2. Materials and methods

2.1. Study area

The surveyed area is approximately 660 km^2 with a mean depth of 15 m (Fig. 1). Several small rivers, notably the Xin'an River, Qinshui River, Yuniao River and Yangting River run into the coastal waters. The area is dominated by semi-diurnal tides, and climate is mainly controlled by the East Asian Monsoon (Chen, 2009). Moreover, the environmental conditions in the area are significantly affected by scallop farming activities. For example, P concentration in the research area has been found significantly higher than that in most of the other coastal waters in China (Yang et al., 2020a). Generally, hypoxia in the bottom water starts to develop in early summer, and reaches the strongest sate in August, but gradually disappears in autumn (Yang and Gao, 2019).

2.2. Sampling and analysis

Two field surveys were conducted at 24 stations in August (summer) and November (autumn) 2017 (Fig. 1). A stainless steel box sampler was used for the sediment sampling, and the top 0–2 cm sediment of each site was collected from the center part of the sampler, gathered in de-aired bags and then frozen at −20 °C. The bottom water collection information and analytical methods, including salinity, temperature, chlorophyll *a* (Chl *a*), DO, dissolved inorganic phosphorus (DIP) and nitrogen (DIN) can be seen in Yang et al. (2020a). Briefly, water salinity, temperature, Chl *a* and DO were determined using a CTD and a YSI sensors with the limits of ±0.01 for salinity, ±0.05 °C for temperature, ± 0.01 μg l^{-1} for Chl *a* and ± 0.1 μmol l^{-1} for DO. DIP and DIN, including ammonium (NH_4^+), nitrite (NO_2^-) and nitrate (NO_3^-) were measured using a SEAL Analytical autoanalyzer. In detail, DIP was measured by ammonium molybdate spectrophotometry; NH_4^+ was measured by spectrophotometric method with salicylic acid; NO_2^- was determined by the azo-dye method; NO_3^- was measured by the cadmium reduction method followed by the azo-dye method; DIN was calculated by the sum of NH_4^+, NO_2^- and NO_3^-. The detection limit was 0.02 μmol l^{-1} for NO_3^- and NO_2^-, and 0.03 μmol l^{-1} for NH_4^+, and 0.01 μmol l^{-1} for DIP.

A fragment of each well mixed sediment sample was centrifuged to extract pore water for DIN and DIP analysis. After that, a part of the sample was used for grain-size analysis, and the remaining part was freeze-dried, homogenized, ground and then sieved through a 200 mesh screen for the subsequent analysis of organic carbon (OC), calcium carbonate ($CaCO_3$) and sedimentary P. The sediment grain size determination was performed with a Mastersizer 2000 laser particle size analyzer, and the results were classified as <4, 4–63 and > 63 μm for clay, silt and sand (Yang et al., 2018). The OC contents were analyzed with an Elementar vario MACRO cube CHNS analyzer with the precision of ±0.02% C by dry weight (n = 5). The $CaCO_3$ content was measured through carbon dioxide gas quality method according to Programme and Rantala (1992). Briefly, approximately 5 g of the sediment was placed in a pre-weighed flask with stopper and treated with 4 mol l^{-1} HCl. The loss of weight due to the evolved CO_2 was determined, and then the $CaCO_3$ content was calculated.

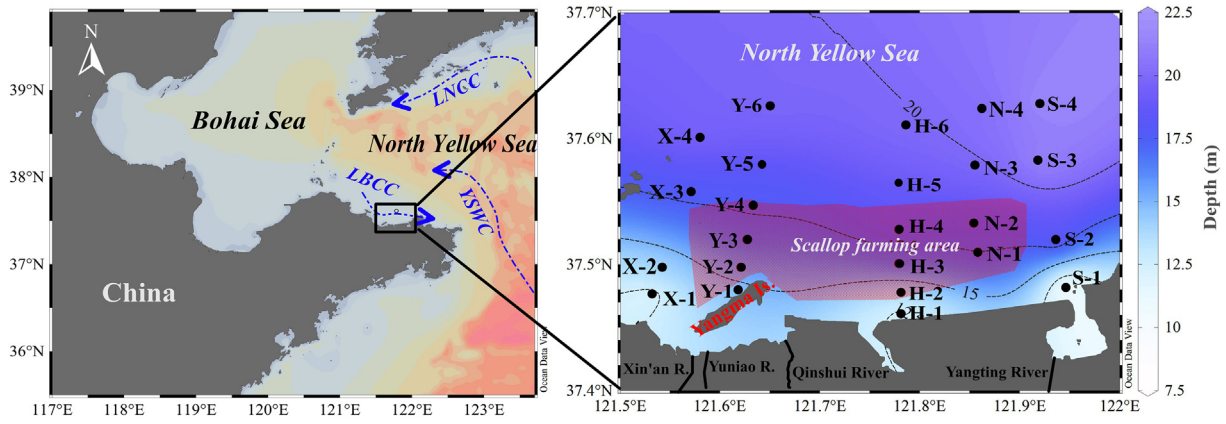

Fig. 1. Sampling sites in the coastal waters around the Yangma Island. The LNCC, LBCC and YSWC represent the Liaonan Coastal Current, Lubei Coastal Current and Yellow Sea Warm Current, respectively.

Sedimentary P was fractionated into five forms according to the SEDEX procedure described in Ruttenberg (1992), i.e. Ex-P, Fe—P, Ca—P, De-P and OP. Briefly, Ex-P was obtained by extraction using 1 mol l^{-1} $MgCl_2$; Fe—P was obtained using citrate-bicarbonate-dithionite (0.22 mol l^{-1} sodium citrate, 0.14 mol l^{-1} sodium dithionite, 1.0 mol l^{-1} sodium bicarbonate); Ca—P was obtained by extraction with acetate buffer; De-P was obtained using 1 mol l^{-1} HCl. Finally, OP was calculated as the difference between extractable P with 1 mol l^{-1} HCl before and after 2 h ignition at 550 °C of the sediment samples. Inorganic P (IP) and total P (TP) were calculated as the sum of the former four forms and all forms of P. The content of P was measured with a PerkinElmer Optima 7000 DV ICP-OES. The detection limit for P was 0.0003–-0.003 μmol g^{-1}. Two marine sediment standard reference materials of China, i.e. GBW-07314 and GBW-07333, were used for quality control of the experimental process. The measured TP contents for materials of GBW-07314 and GBW-07333 were 20.7 ± 0.7 and 16.2 ± 0.4 μmol g^{-1}, which were well consistent with the standard values of these two sediments (20.8 ± 2.0 and 17.1 ± 1.1 μmol g^{-1} for GBW-07314 and GBW-07333).

2.3. Incubation experiment

For the study of potential P-release fluxes at the sediment-water interface in August and November, the sediment samples at stations Y-2, Y-4, Y-6, H-2, H-4 and H-6 were incubated in lab for 3 days with artificial seawater under simulated field conditions (Table S1 in Supplementary Information). According to the field conditions in the overlying water, the artificial seawater was prepared by adding appropriate amounts of NaCl, $NaNO_2$, KNO_3, $(NH_4)_2SO_4$, $NaHCO_3$, KH_2PO_4 and Na_2SiO_4, and then its pH was regulated using 0.1 mol l^{-1} HCl or NaOH solution. The DO content in the water was regulated by pumping different ratios of air and nitrogen into the incubation bottles (Gao, 2019).

Approximately 200 g wet sediment samples were placed in plexiglass culture bottles, and then filled with 450 ml artificial seawater. Subsequently, the simulation experiments were performed under dark condition in biochemistry incubators. Timing was started after the experiments stabilized for 3 h, and 20 ml water sample was collected from each culture bottle after 0, 4, 8, 12, 24, 36, 48, 60 h, respectively. Then, the same volume of artificial seawater was added back to each culture bottle after sampling. The P-release fluxes were estimated by quantifying the changes in DIP over time. More details about the simulation experiments and analysis methods of diffusive flux of DIP were described by Gao (2019). Moreover, after 60 h, the sediment in culture bottles was pretreated with the methods in Section 2.2 for the subsequent analysis of sedimentary P.

2.4. Data processing

Contour maps for the parameters of DO, sedimentary P fractions, OC, $CaCO_3$ and the clay, silt and sand fractions of sediments were generated with the Ocean Data View 4. Data processing and statistical analysis were performed with the SPSS 19.

3. Results

3.1. General characteristics of the bottom and pore waters

Overall, the bottom-water salinity was relatively stable, while the temperature ranged widely from 11.5 to 25.9 °C. Spatially, the salinity was lower in the inshore part than offshore part. The high values of temperature were observed in the inshore part in August and eastern region in November (Table S1 and Fig. S1).

As for bottom-water DO, its values varied from 55.0 to 240.1 μmol l^{-1}. In August, the hypoxia spots, i.e. DO <93.0 μmol l^{-1}, were formed, which accounted for ~30% of the study area, whereas the DO concentration was >200 μmol l^{-1} in November. Notably, in August, the relatively low DO concentrations appeared right in the scallop-farming area (*SFA*) (Fig. S1e).

The concentrations of NO_3^-, NO_2^-, NH_4^+ and DIP in the bottom water ranged broadly from 0.22 to 26.06, 0.10 to 0.41, 0.46 to 16.20, and 0.17 to 1.86 μmol l^{-1}, respectively (Table S1). On the whole, the high values of DIN and DIP were all observed in the inshore part, except for DIP in November (Fig. S1).

For the pore water, the concentrations of NO_3^-, NO_2^-, NH_4^+ and DIP in August ranged from 7.72 to 11.83, 1.62 to 3.62, 122.4 to 328.3, and 0.98 to 2.40 μmol l^{-1}, respectively (Table S1). The concentrations of NO_3^- and NO_2^- in November were equivalent to those in August. However, the concentrations of NH_4^+ and DIP in November were significantly lower than those in August, varying from 24.50 to 65.70, and 0.29 to 0.76 μmol l^{-1}, respectively.

3.2. Surface sediment characteristics

The sediments were mainly composed of clayey silt and sandy silt (Fig. S2); only the sediment in the Site S-1 near the Yangting River mouth was composed of sand (Fig. S3). On average, the clay fraction in August was about 49% higher than that in November, while the sand fraction in August was about 32% lower than that in November (Table S2). Spatially, the clay and silt percentages were lower in the inshore zone than offshore zone, which was opposite to the distributions of sand in these two months (Fig. S3a–f). Besides, sediments in the *SFA* were significantly finer (mean 35.4 ± 9.9% of clay) than those in the non-scallop-farming area (*NSFA*) (mean 19.1 ± 12.1% of clay) in August

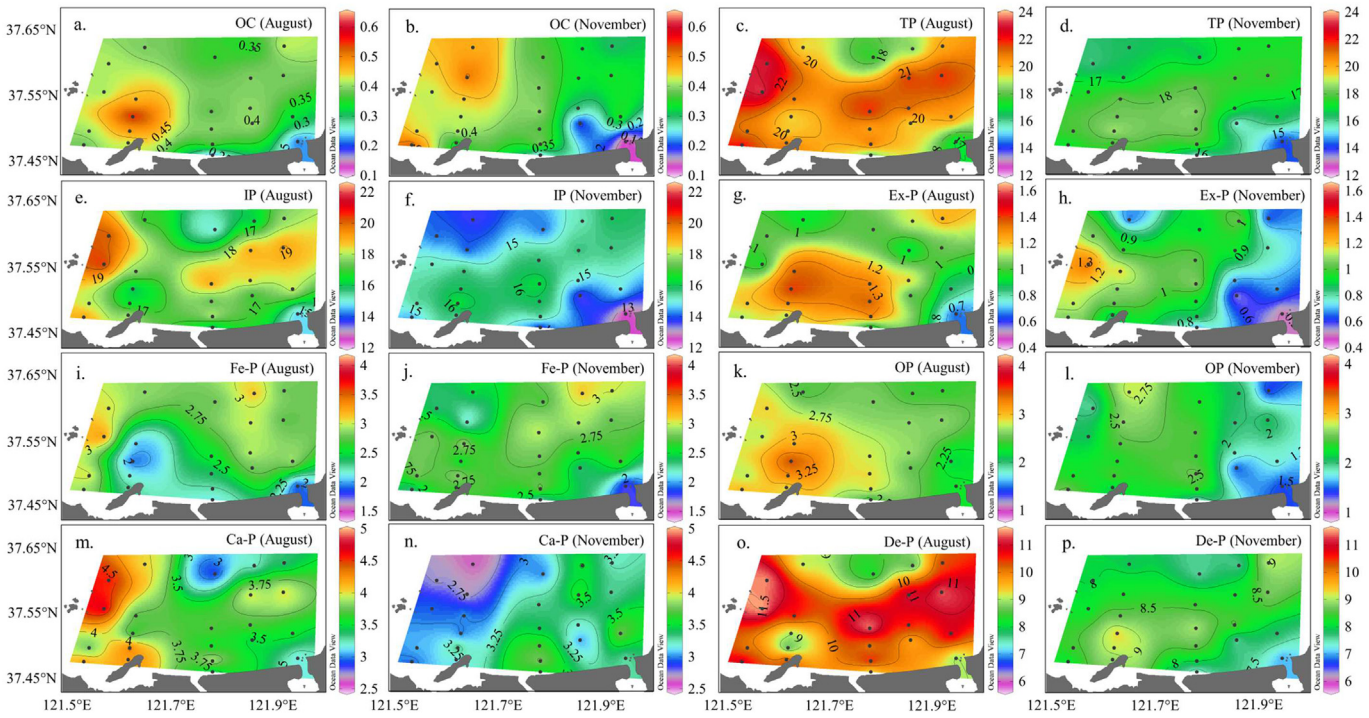

Fig. 2. Spatial variations in the contents of sedimentary OC (%) and P forms (μmol g^{-1}) in August and November.

(Fig. S3a). The $CaCO_3$ contents varied from 0.18 to 7.16 (Table S2), and its contents in the *SFA* were significantly higher than those in the *NSFA* (Fig. S3g and h).

The OC contents ranged from 0.08 to 0.64% with the mean values of 0.39 ± 0.10% in August and 0.37 ± 0.13% in November (Table S2). The distribution patterns of OC were roughly similar in the two months, increasing from the inshore regions to the offshore regions (Fig. 2a and b). In addition, the average OC value in August was higher in the *SFA* (0.45 ± 0.08%) than that in the *NSFA* with the average value of 0.35 ± 0.09%, while no significant difference of OC in *SFA* and *NSFA* was found in November.

3.3. Total P and its fractions in the surface sediments

TP contents varied from 13.42 to 23.88 μmol g^{-1}. As the main component of TP, IP contents varied from 12.12 to 21.19 μmol g^{-1} (Table S2). The SEDEX results indicate that De-P was the most predominant P pool with the average contents of 10.13 ± 1.47 and 8.24 ± 0.85 μmol g^{-1} in August and November followed by Ca—P (mean 3.76 ± 0.58 and 3.20 ± 0.41 μmol g^{-1}), Fe—P (mean 2.62 ± 0.51 and 2.63 ± 0.52 μmol g^{-1}) and OP (mean 2.71 ± 0.41 and 2.15 ± 0.52 μmol g^{-1}). The contents of Ex-P were the lowest with the mean values of 1.10 ± 0.26 and 0.90 ± 0.27 μmol g^{-1} in August and November (Table S2). For bioavailable P (Bio—P, the sum of Ex-P, Fe—P and OP), its values ranged from 4.65 to 7.08 μmol g^{-1} in August and 3.43 to 7.18 μmol g^{-1} in November, which accounted for 28.0–37.4% and 25.4–38.3% of TP in corresponding months, respectively.

Fig. 2c–p show the spatial variations of TP and its fractions. During the investigation, the lowest contents of TP and P fractions were all observed in the Site S-1 near the Yangting River mouth except for the Ca—P in November. In August, the high values of TP, IP, Fe—P and Ca—P were recorded in the western area; while relatively higher

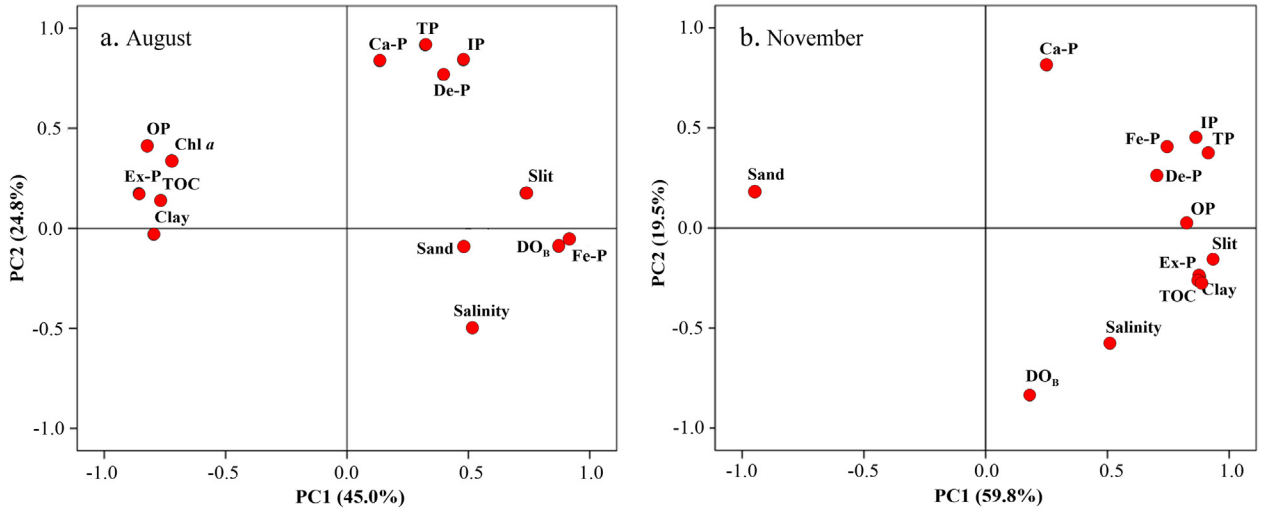

Fig. 3. PCA loadings for different sedimentary P forms and relevant environmental parameters. Subscript B represents the bottom water.

contents of Ex-P and OP occurred near the Yangma Island, which was similar to the distributions of OC and clay. In addition, the OP and Ex-P in the *SFA* were significantly higher than those in the *NSFA*, which was opposite to the distribution of Fe—P (Fig. 2). In November, relatively high contents of TP, IP, Ex-P and OP were observed in the western zone (Fig. 2d, f, h and l), which was opposite to the distribution of Ca—P (Fig. 2n). However, no significant spatial distribution pattern of the other P fractions was observed (Fig. 2).

3.4. Benthic DIP flux

The benthic DIP fluxes were 2.17 ± 1.17 μmol cm^{-2} yr^{-1} (0.76 to 3.56 μmol cm^{-2} yr^{-1}) in August and − 1.53 ± 0.47 μmol cm^{-2} yr^{-1} (−1.88 to −0.78 μmol cm^{-2} yr^{-1}) in November (Fig. S5). The results indicate that the sediment could release DIP in August, but absorb DIP in November. Spatially, the highest flux was observed at station H-2 in August, and the lowest value appeared at station Y-2 in November (Fig. S5).

3.5. Correlation and principal component analysis

As shown in Table S3, in August, Fe—P had a significant positive correlation with DO concentration in the bottom water (DO_B) and silt fraction of sediment with the Pearson's correlation coefficient (r) of 0.880 ($P < 0.001$) and 0.602 ($P < 0.01$), respectively, indicating that the silt fraction of sediment and oxygen-rich condition in the bottom water were beneficial for the Fe—P accumulation; the clay and silt fractions of sediment had significant positive correlations with OC, Ex-P and OP, reflecting the importance of fine-grained sediment in the binding of OM and P fractions. In November, all P fractions except Ca—P had significant positive correlation with fine-grained fractions of sediment (clay and silt), which was similar to that in August to some extent (Table S3).

Two principal components, i.e. PC1 and PC2, were distinguished, which explained 69.8% in August and 79.3% in November of the total variance, respectively. In August (Fig. 3a), PC1, which accounted for 45.0% of the total variance, had high positive loadings for DO_B, silt fraction of sediment, salinity and Fe—P, reflecting the importance of DO_B and sediment type to Fe—P. Negative loadings of PC1 were found for Chl *a*, clay, OC, Ex-P and OP, which reflects the relationship between marine OM and its related environmental factors. PC2 accounted for 24.8% of the total variance with high positive loadings for TP, IP, Ca—P and De-P. In November (Fig. 3b), PC1 explained 59.8% of the total variance with high positive loadings for OC, TP, IP, Fe—P, Ex-P, OP, De-P and clay and silt fractions of sediment but negative loading for sand fraction of sediment. PC2 accounted for 19.5% of the total variance with high positive loadings for Ca—P and negative loading for DO_B, which indicates that hypoxia may contribute to Ca—P enrichment.

4. Discussion

4.1. Characteristics of P content in sediments

As shown in Table 1, the TP contents in this study, 20.32 ± 2.21 μmol g^{-1} in August and 17.12 ± 1.79 μmol g^{-1} in November, were comparable to those observed in the Laizhou Bay, the East China Sea and the Zhejiang offshore area, and higher than those observed in the North Yellow Sea, the Daya Bay, the Zhangzi Island coastal waters and the Haizhou Bay, but lower than those in the Admiralty Bay. Based on the quality assessment standards of the Department of Environment and Energy, Canada, if the content of sedimentary P exceeds 19.4 μmol g^{-1}, it could lead to potential ecological risks (Mudroch and Azcue, 1995; Barik et al., 2019). Accordingly, ~59% of the surveyed sites were at potential ecological risks in August.

In addition, the results suggest that IP was the main form of TP, which was consistent with other studies, such as Fang et al. (2007), He et al. (2010), Zhuang et al. (2014) and Zhou et al. (2016). In terms

Table 1
Comparison of the contents of sedimentary P in the present study with these in some other marginal seas reported in the literature (μmol g^{-1}). It should be noticed that the sequential extraction methods used in the cited literature are not exactly the same as in this study.

Location	Time	TP	IP	Ex-P	Fe-P	Ca-P	De-P	OP	Bio-P	Reference
North Yellow Sea	Oct. 2007	6.50 ± 0.08	n.d.	0.56 ± 0.01	0.36 ± 0.01	2.11 ± 0.04	2.38 ± 0.01	0.55 ± 0.01	n.d.	Meng et al. (2012)
Yellow Sea and East China Sea	2006	n.d.	n.d.	0.2	1.00	4.69	1.97	1.09	n.d.	Zhang et al. (2013c)
East China Sea		17.47 ± 1.93	14.73 ± 1.49	1.45 ± 0.26	n.d.	1.00 ± 0.28	12.27 ± 1.65	2.75 ± 1.13	n.d.	Fang et al. (2007)
East China Sea inner shelf	Jul.–Aug. 2011	17	n.d.	0.43	0.43	3.03	9.45	2.73	n.d.	Meng et al. (2014)
East China Sea shelf	May–Jun. 2014	14.3 ± 1.14	11.24 ± 1.27	0.46 ± 0.17	0.43 ± 0.25	4.95 ± 1.48	5.10 ± 1.86	3.06 ± 0.72	4.25 ± 1.05	Zhou et al. (2016)
Zhejiang offshore	Apr. 2009	18.16 ± 4.38	n.d.	0.21 ± 0.05	3.11 ± 0.92	0.41 ± 0.09	9.83 ± 1.17	2.22 ± 0.85	n.d.	An et al. (2012)
Daya Bay	Aug. 2007	11.40 ± 0.26	9.69 ± 0.27	0.66 ± 0.73	0.91 ± 0.37	3.10 ± 0.32	4.26 ± 0.40	1.70 ± 0.81	n.d.	He et al. (2010)
Laizhou Bay	Oct. 2011	16.19	14.09	0.36	1.06	2.01	10.67	2.07	3.48	Zhuang et al. (2014)
Zhangzi Island coastal waters	Nov. 2011	9.19	7.43	0.44	1.10	1.05	4.85	1.64	3.17	Zhuang et al. (2014)
Haizhou Bay	Aug. 2014	14.06	9.56	0.17	0.38	2.49	6.52	4.69	5.19	Gao et al. (2015)
Admiralty Bay	May 2004	32.31 ± 4.29	n.d.	1.56 ± 0.57	4.20 ± 2.45	11.77 ± 3.00	13.09 ± 4.15	1.69 ± 0.51	19.22 ± 4.91	Berbel and Braga (2014)
Bothnian Sea	2012–2013	n.d.	n.d.	2.03	44.69	15.89	3.63	10.24	n.d.	Egger et al. (2015)
Coastal waters around the Yangma Island	Aug. 2017	20.32 ± 2.21	17.61 ± 2.11	1.10 ± 0.26	2.62 ± 0.51	3.76 ± 0.58	10.13 ± 1.47	2.71 ± 0.41	6.39 ± 0.75	This study
	Nov. 2017	17.12 ± 1.79	14.97 ± 1.49	0.90 ± 0.27	2.63 ± 0.52	3.20 ± 0.41	8.24 ± 0.85	2.15 ± 0.52	5.65 ± 1.15	

n.d.: no data.

of different forms of P, overall, their contents were comparable to those observed in the East China Sea shelf and the Laizhou Bay, but higher than those in the North Yellow Sea, the Daya Bay and the Zhangzi Island coastal waters (Table 1).

4.2. Effect of hypoxia on P recycling and transformation

In August, the studied sites Y-2, Y-3, Y-4, H-1, H-2 and S-2 were covered by hypoxic water (Fig. S1e). In November, the bottom hypoxia disappeared under the influence of low temperature and strong hydrodynamic conditions (Yang et al., 2020a). Thus, the contrasting DO conditions in the bottom water in August and November make the study area an ideal region for the study of the effects of hypoxia on P biogeochemical cycle.

4.2.1. DIP in the bottom and pore waters

As shown in Table S1, the concentrations of DIP and NH_4^+ in the bottom and pore waters in August increased significantly compared with those in November. Spatially, the concentrations of DIP together with NH_4^+ in the bottom and pore waters in the hypoxic zone were significantly higher than those in the oxygen-rich region in August (Fig. S1 and Table S1). Thus, DIP in the bottom and pore waters was significantly positively correlated ($P < 0.05$), and they both had negative correlations with the bottom DO in August (Table S4). These results support the claim that large amounts of DIP can be potentially released into water via sediments under hypoxic conditions, which plays a key role in regulating the concentrations of DIP in the water column (Liu et al., 2016, 2020).

4.2.2. Sedimentary P dynamics

In this study, TP content in August was significantly higher than that in November (Table S2). Judging from the structural variations of sedimentary P (Fig. S6), the percentages of OP and De-P in August were significantly higher than those in November, which were contrary to the changes of Fe—P. Spatially, the Ex-P and OP contents in the hypoxic zones in August were significantly higher than those in the oxygen-rich regions, which were contrary to the distribution of Fe—P (Fig. 2). Therefore, these forms of P and bottom DO all showed significant correlations (Table S3), indicating that the bottom DO was an important factor affecting these P dynamics.

It is widely known that some P can be easily released into the overlying water via the dissolution of Fe/Mn (oxy) hydroxides under hypoxic environments (Kraal et al., 2012). Hence, the relatively low Fe—P content observed in August may be related to decreased Fe oxides due to low DO level (Figs. 2i and S1e), as further supported by the significant positive correlation between Fe—P and bottom DO ($P < 0.001$) (Table S3). In addition, low DO can promote the conversion of Fe—P to Ex-P in sediment (Zilius et al., 2015; Liu et al., 2020), thereby leading to the increase in Ex-P content, as supported by the negative correlation between Fe—P and Ex-P (Table S3). Similar results were found in other estuarine systems (Gu et al., 2019). However, no significant correlation between Fe—P and DO was observed in November, which may be caused by strong winds and coastal hydrodynamic conditions, thereby supplementing the DO of the overlying water (Fig. S1).

OP is generally an important source of P to the marine sediment surface, especially under anoxic conditions due to the inhibition of OM aerobic degradation (Picard et al., 2019). During the investigation, the highest OP content of 3.77 μmol g^{-1} was found in the organic-rich (average OC content of 0.64%), strongly hypoxic sediments at site Y-3 (average DO of 59.7 μmol l^{-1}) in August (Fig. 2k). However, the investigation area in November was in aerobic condition, which was helpful for the degradation of OM, resulting in a decrease in OP content in sediment (Table S2).

4.2.3. Decomposition and transformation of P in sediment

The OC/OP ratio of marine algae is ~106, and it is generally ascribed to the influence of terrestrial surface input or preferential regeneration of P relative to C if the OC/OP ratio in marine sediment is higher than 106 (Redfield, 1963; Meng et al., 2014). In this study, the OC/OP ratio was 118 ± 23 in August (Table S2 and Fig. 4a), which was roughly consistent with the marine phytoplankton source. However, the value of OC/OP was 139 ± 38 in November (Table S2 and Fig. 4a), which was significantly higher than that in August. Previous study has found that the SOM were mainly derived from marine algae in the study area (Yang et al., 2018). In August, hypoxia occurred in the bottom water; thus, the decomposition of OM was inhibited to a certain extent and excess OM from the primary producers could be preserved in the sediment (Yang et al., 2018; Picard et al., 2019). This partly explains why the OC/OP ratio was lower in August than that in November.

Generally, most of the reactive P at the sediment-water interface exists in the OM form. Before permanent burial, part of the OM is prone to decomposition accompanied by the release of large amounts of DIP. Thus, the higher DIP concentrations were found in the bottom water than in the surface water in August and November (Fig. S1). In addition, part of the regenerated DIP by OM mineralization could be absorbed to clay minerals, bind to iron oxides, combine with $CaCO_3$ or diffuse to the sediment-water interface and escape into the water column (Cha et al., 2005; März et al., 2014). As can be seen in Table S3, significant correlations between OP and Ex-P were found in August ($P < 0.001$) and November ($P < 0.01$) (Table S3), indicating that part of the regenerated P

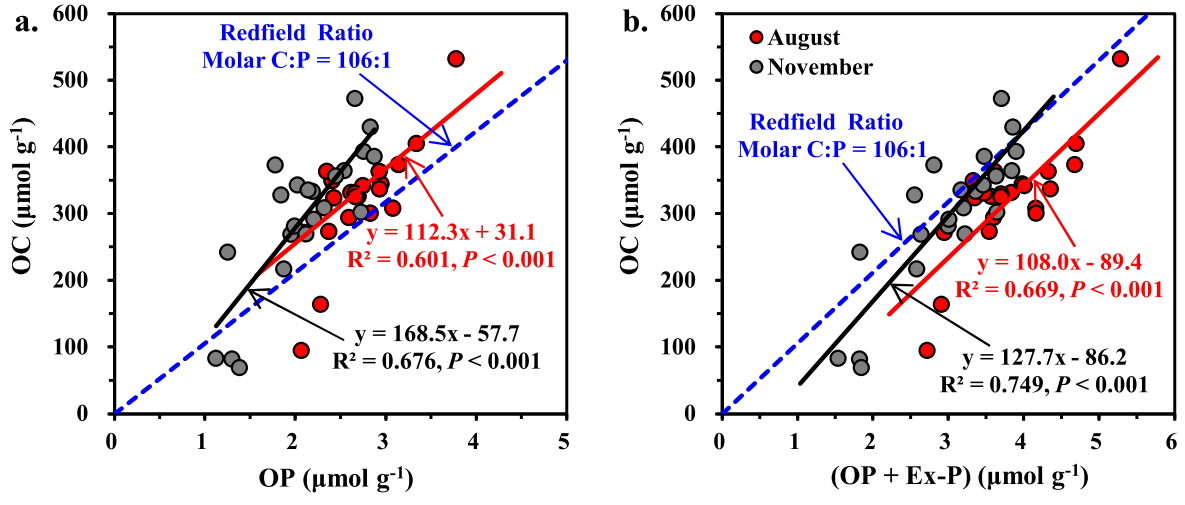

Fig. 4. Relationships between the OC and OP and (OP + Ex-P) contents in the surface sediments.

was adsorbed to clay minerals. That is to say, OC/(OP + Ex-P) could be closer to the Redfield Ratio than that of OC/OP. Therefore, OC/(OP + Ex-P) could be a better indicator for explaining the behavior of sedimentary P. In August and November, the OC/(OP + Ex-P) ratios, 83 ± 18 and 96 ± 28, respectively, were much lower than 106, indicating the presence of excess (OP + Ex-P) relative to OC.

In addition, based on the difference between monthly average of Ex-P and the linear intercept between OC and (OP + Ex-P), the Ex-P content produced by OP decomposition was estimated (Fig. 4b). In August and November, the produced Ex-P contents were ~0.27 and ~0.23 μmol g^{-1}, respectively, accounting for ~24.5% and ~25.5% of the corresponding total Ex-P. Notably, the calculated Ex-P content had a certain deviation from the real condition due to the transformation of reactive P phases during burial processes.

4.2.4. Benthic P dynamics and their underlying mechanisms

Bio-P content can reflect the degree of pollution and the internal P release ability of sediment (Zhou et al., 2016; Yang et al., 2019). During the investigation, the Bio-P contents were 6.39 ± 0.75 μmol g^{-1} in August and 5.65 ± 1.15 μmol g^{-1} in November accounting for 31.9 ± 3.3% and 32.9 ± 4.0% of corresponding TP (Table S2), which were slightly higher than those in the East China Sea shelf (Zhou et al., 2016), but lower than those in the Admiralty Bay (Berbel and Braga, 2014).

The benthic DIP fluxes were 2.17 ± 1.17 and − 1.53 ± 0.47 μmol cm^{-2} yr^{-1} in August and November, respectively (Fig. S5). The benthic DIP fluxes in August were higher than some coastal waters listed in Table 2, e.g. the Rushan Bay, the Baltic Sea, the Jiaozhou Bay and the Iberian Margin (NE Atlantic), but lower than those in the hypoxic areas of the Yangtze River Estuary and the North-western coast of Baltic Proper. It was reported that the accumulation rate of sediment in the southern coastal area of the NYS close to the study area ranged from 0.56– 1.18 g cm^{-2} yr^{-1} with an average of 0.87 g cm^{-2} yr^{-1} (Qi et al., 2004; Wang et al., 2013). Therefore, approximately 2.49 ± 1.34 μmol g^{-1} of P could be recycled back into the water column in August, corresponding to ~39% of Bio—P. In contrast, approximately 1.76 ± 0.54 μmol g^{-1} of DIP might be buried in sediment, corresponding to ~31% of Bio-P in November.

In August, the benthic DIP flux was significantly correlated with OP ($P < 0.001$); however, it had a negative correlation with Fe—P ($P < 0.001$) (Fig. S7), which was different from these reported in Zhang et al. (2012), Adhikari et al. (2015) and Yang et al. (2020b). This could be mainly controlled by DO conditions in environment. In this study, the sediments with low Fe—P contents were from the sampling sites in the low DO areas (Figs. 2i and S1e), thus leading to a negative correlation between benthic DIP flux and Fe—P. Besides, the benthic DIP flux was significantly positively correlated with the Ex-P ($P < 0.001$) and Ca—P ($P < 0.05$) in August (Fig. S7), indicating that the increasing DIP of pore waters promoted the formation of Ex-P and Ca—P. Indoor incubation experiment further supported the above conclusion, that is, the content of Fe—P and OP decreased by 38.7% and 18.3%, respectively, after the experiment; however, the Ex-P content increased by 28.6% compared with that before the experiment.

In November, the investigation area was in oxygen-rich conditions. Therefore, most of regenerated DIP by OM mineralization was scavenged by ferric iron oxides and/or adsorbed to clay minerals in surface sediments (Mort et al., 2010). This could be the main reason for no significant correlations between benthic DIP flux and sedimentary P forms in November (Fig. S8). Furthermore, the incubation experiment results show that the OP content lost 23.7% compared with the value before experiment, while the Ex-P and Fe—P contents increased by 62.3% and 10.7%, respectively.

Overall, it can be concluded that OP and Fe—P could be the main fractions of internal P-release in the hypoxia season. Incubation experiment results indicate, in August, ~0.92 μmol g^{-1} of Fe—P and ~0.52 μmol g^{-1} of OP could be transformed to DIP and released into water, which was consistent with the results reported in the Rushan Bay (Liu et al., 2016a) and the coastal area of the Changjiang Estuary (Liu et al., 2020). However, ~0.36 μmol g^{-1} of DIP was adsorbed to clay minerals in August. Different from the former, in November, ~0.54 μmol g^{-1} of OP was converted into DIP, while ~0.55 and ~0.28 μmol g^{-1} of DIP was adsorbed to clay minerals and bind to iron oxides.

4.3. Effects of scallop farming on sedimentary P cycle

In August, the hydrodynamic conditions were relatively weak, which accelerated the deposition of particulate OM, especially in the *SFA*. This partly explains why the sedimentary TP content in August was significantly higher than that in November (Table. S2). Spatially, the OP and Ex-P contents in the *SFA* were significantly higher than those in the *NSFA* in August (Fig. 2). Generally, scallop farming can increase fine particles and biological debris in sediments, thereby promoting the deposition of OP and increasing in the Ex-P adsorption and regeneration (Zhang et al., 2013a, 2013b), as supported by the significant positive correlations between Ex-P and clay, and OP and clay in August ($P < 0.001$) (Table S3).

On the contrary, the Fe—P content in the *SFA* was significantly lower than that in the *NSFA*. In fact, the Fe—P was mainly controlled by the redox conditions. Scallop farming activities also played an important role in this process (Kraal et al., 2012). This is because scallop farming can promote the formation of hypoxia in the bottom water (Yang et al., 2020a). As shown in Fig. S1, the bottom DO concentration in the

Table 2
Comparison of the benthic DIP flux (μmol cm^{-2} yr^{-1}), P burial flux (μmol cm^{-2} yr^{-1}) and burial efficiency (%) of P of surface sediments in the present study with these in some other marginal seas reported in the literature. The positive and negative values represent the release of P from sediment to overlying water and the transfer of P from overlying water to sediment, respectively.

Location	Time	Benthic DIP flux	P burial flux	P burial efficiency	Reference
Yellow Sea	1998–1999	−0.086 ± 0.031	2.60 ± 1.79	ca. 100	Liu et al. (2004)
Bohai Sea	1998–1999	−1.1 ± 0.4	9.04 ± 10.0	ca. 100	Liu et al. (2004)
East China Sea middle shelf		0.558 ± 0.481	6.78 ± 5.84	92.4 ± 1.2	Fang et al. (2007)
Yangtze River Estuary and adjacent coast	2003–2004	3.30 ± 2.82	21.7 ± 23.2	84.3 ± 3.	Hou et al. (2009)
East China Sea	Oct. 2012	0.50 ± 0.52	14.25 ± 5.97	97 ± 2	Yang et al. (2017)
Jiaozhou Bay	2001–2003	1.01	n.d.	91	Qi et al. (2011)
The coastal area of Rushan Bay	May 1999	1.02 ± 0.63	29.96	82.6	Liu et al., 2016a
Baltic Sea	2002, 2005	1.25 ± 0.56	n.d.	n.d.	Viktorsson et al. (2012)
Iberian Margin (NE Atlantic)	May 1999	0.302 ± 0.329	14.79 ± 11.61	94 ± 7	van der Zee et al. (2002)
South-eastern coast of India	May 2004	0.163 ± 0.061	6.38 ± 0.93	99.83 ± 0.21	Prasad and Ramanathan (2010)
North-western coast of Baltic Proper	Nov. 2008	4.92 ± 2.55	6.77 ± 1.69	60 ± 6	Rydin et al. (2011)
Great Barrier Reef Continental Shelf		0.067 ± 0.148	3.0 ± 2.9	95 ± 8	Monbet et al. (2007)
Coastal waters around the Yangma Island	Aug. 2017	2.17 ± 1.17	17.66 ± 2.08	89.5 ± 4.57	This study
	Nov. 2017	−1.53 ± 0.47	14.87 ± 1.70	ca. 100	

n.d.: no data.

SFA, on average, was ~40 μmol l^{-1} lower than that in the *NSFA*, which promoted the conversion of Fe—P to Ex-P and DIP (Zilius et al., 2015).

For Ca—P and De-P, their spatial distributions were not significant in August. Generally, scallop farming activities can increase the $CaCO_3$ content in the sediments (Fig. S3 g and h), which may lead to an increase in Ca—P content (Zhang et al., 2013a). However, the Ca—P in this study was mainly controlled by the DIP concentration in the pore waters, which was supported by the significant positive correlation between pore-water DIP and Ca—P in August (Table. S4). In addition, part of DIP derived from OP and Fe—P may also precipitate into Ca—P (Meng et al., 2015), which could be another source for the increase of Ca—P. For De-P; the most abundant De-P was found in the western zone of the study area in August, which was probably related to the terrestrial inputs (Ruttenberg and Berner, 1993).

In November, the investigation area was significantly affected by strong winds and coastal currents; thus, strong resuspension process of surface sediment appeared in November (Yang et al., 2018). Therefore, sedimentary clay fraction in November was obviously lower than that in August, which reduced the storage of some P, e.g. Ex-P and OP (Table S2). Moreover, strong hydrodynamic conditions promoted the re-oxygenation process in the bottom water, thereby accelerating the decomposition of OP and the generation of Fe—P (Table S2). Spatially, the OC, Ex-P, Fe—P, Ca—P, De-P and OP in the *SFA* were slightly higher than those in the *NSFA* by 6.0, 10.0, 8.6, 6.7, 9.9 and 11.8%, respectively (Fig. 2). This is because scallop farming activities can reduce hydrodynamic conditions in the *SFA*, thereby beneficial to the preservation of sedimentary P.

To further assess the impact of scallop farming on the P dynamics, we roughly estimated the contribution of bio-deposited P (mainly OP) to sedimentary P. According to the research of Niu (2014), the daily production of biodeposits by the scallops in summer and autumn were about 1.80 and 1.52 μmol ind^{-1}, respectively. Generally, the annual output of scallops is ~5 × 10^9 ind (Yang et al., 2020a). Thus, the rate of biodeposited P excreted by scallops was ~1.20 and ~1.01 μmol cm^{-2} yr^{-1}, respectively in August and November. Based on this calculation, the biodeposited P rate by the scallops in the surveyed area accounted for 44.3% and 50.3% of the OP burial fluxes (2.64 and 2.01 μmol cm^{-2} yr^{-1} according to the formula of $F = c \times \omega$ in Section 4.4), respectively. This further proves scallop biodeposition may be one of the main sources of OP in the surveyed area.

4.4. Sedimentary P burial and budget

The P removed from the water is mainly buried in the sediment. P burial fluxes (F, μmol cm^{-2} yr^{-1}) were calculated using the following formula, $F = c \times \omega$, where c (μmol g^{-1}) is the mean sedimentary P content, ω is the accumulation rate of sediment in g cm^{-2} a^{-1} (Ingall and Jahnke, 1994). In this study, the F of the TP (P_{Total}) ranged from 11.67 to 20.78 μmol cm^{-2} yr^{-1} with the mean values of 17.66 ± 2.08 μmol cm^{-2} yr^{-1} in August and 14.87 ± 1.70 μmol cm^{-2} yr^{-1} in November, which were significantly higher than those found in most marginal seas listed in Table 2, but comparable to those previously reported in the East China Sea (Hou et al., 2009; Yang et al., 2017) and the Iberian Margin (van der Zee et al., 2002).

The P burial efficiency (*PBE*), which was determined based on the formula of $PBE = F / (F + \text{benthic DIP flux}) \times 100\%$, has been widely used to evaluate the burial capacity of P in sediments (van der Zee et al., 2002). In this study, the benthic DIP fluxes were 2.17 ± 1.17 μmol cm^{-2} yr^{-1} in August and −1.53 ± 0.47 μmol cm^{-2} yr^{-1} in November as shown in Section 3.4. Therefore, the *PBE* was 89.5 ± 4.6% in August and 100% in November, which was in good agreement with the previous studies listed in Table 2.

In addition, a simple benthic P budget model was established based on the results before and after the incubation experiment (Fig. 5). The P budget results indicate that Ex-P, OP and Fe—P were the main forms of reactive P preserved in the sediment. Compared with oxygen-rich

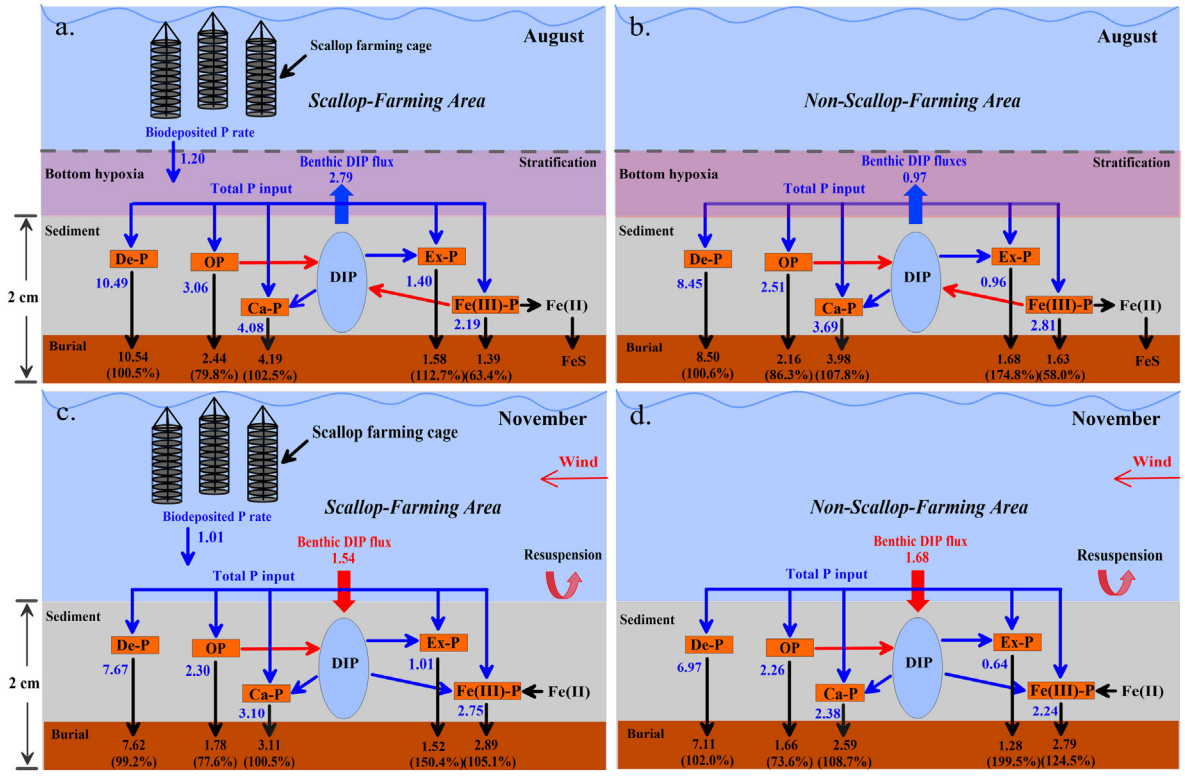

Fig. 5. Sedimentary P budget in the study area. The results were obtained based on sediment investigations combined with the laboratory incubation experiment on the samples from stations Y-2, Y-4, Y-6, H-2, H-4 and H-6. In the figure, the unit of biodeposition P rate and benthic DIP flux is μmol cm^{-2} yr^{-1}; the unit of sedimentary P forms is μmol g^{-1}.

conditions, low oxygen promoted the reductive dissolution of sedimentary Fe—P, while inhibited the decomposition of OP to a certain extent. Scallop farming activities increased the input of OP in sediments, in turn affecting the sedimentary P cycle.

5. Conclusions

Exploring the biogeochemical cycle of sedimentary P in the coastal waters is an important step toward understanding the regional material cycling and environmental evolution and protection. This study revealed the characteristics of sedimentary P cycle and its underlying mechanisms in a coastal water ecosystem with scallop farming activities and seasonal hypoxia. The average percentages of P fractions in TP were in the order of De-P > Ca-P > OP > Fe-P > Ex-P in August and De-P > Ca-P > Fe-P > OP > Ex-P in November. The contents of Ex-P, Ca—P, De-P and OP were generally higher in August than these in November. The mean contents of Bio-P were 6.39 and 5.65 μmol g^{-1} in August and November, respectively, which accounted correspondingly for 31.9% and 32.9% of TP.

Summer hypoxia, scallop farming activities and hydrodynamic conditions were the main factors affecting the sedimentary P cycle. The laboratory incubations combined with situ field investigations results indicate that, in summer, hypoxia significantly facilitated P mobility and release via the mineralization of OM and dissolution of Fe-P; as a rough estimate, ~39% of the Bio-P could be recycled back into the water column. In contrast, the overlying water in autumn returned to oxygen-rich conditions with decreasing temperature and disappearing stratification, and thus greatly promoted the formation of Fe—P via co-precipitation of phosphate with Fe/Mn oxides. Thus, ~1.76 μmol g^{-1} of DIP might be absorbed in sediment in November, corresponding to the ~31% of the sediment stored Bio—P. Furthermore, scallop farming activities also affected the P mobility through biological deposition and reduced hydrodynamic conditions. This study highlighted the significant effects of hypoxia and anthropogenic activities (mariculture activities) on the sedimentary P cycle in coastal waters.

CRediT authorship contribution statement

Bo Yang: Investigation, Formal analysis, Writing - original draft. **Xuelu Gao:** Conceptualization, Resources, Writing - review & editing. **Jianmin Zhao:** Funding acquisition, Writing - review & editing. **Yongliang Liu:** Writing - review & editing. **Tianci Gao:** Investigation. **Hon-Kit Lui:** Writing - review & editing. **Ting-Hsuan Huang:** Writing - review & editing. **Chen-Tung Arthur Chen:** Writing - review & editing. **Qianguo Xing:** Writing - review & editing.

Declaration of competing interest

The authors declare that they have no known competing financial interests or personal relationships that could have appeared to influence the work reported in this paper.

Acknowledgments

This work was financially supported by the Strategic Priority Research Program of the Chinese Academy of Sciences (XDA23050303). The assistance of Dr. Kai Liu in the sample collection and laboratory work is greatly appreciated.

Appendix A. Supplementary data

Supplementary data to this article can be found online at https://doi.org/10.1016/j.scitotenv.2020.143486.

References

Adhikari, P.L., White, J.R., Maiti, K., Nguyen, N., 2015. Phosphorus speciation and sedimentary phosphorus release from the Gulf of Mexico sediments: implication for hypoxia. Estuar. Coast. Shelf Sci. 164, 77–85.
An, M.M., Wang, Y.M., Zheng, A.R., 2012. Study of chemical forms of phosphorus and their distributions in the surface sediment in Zhejiang Offshore. J. Xiamen Univ. Nat. Sci. 51 (1), 77–83.
Barik, S.K., Bramh, S., Bastia, T.K., Behera, D., Mohanty, P.K., Rath, P., 2019. Distribution of geochemical fractions of phosphorus and its ecological risk in sediment cores of a largest brackish water lake, South Asia. Int. J. Sediment Res. 34, 251–261.
Berbel, G.B., Braga, E.S., 2014. Phosphorus in Antarctic surface marine sediments-chemical speciation in Admiralty Bay. Antarct. Sci. 26, 281–289.
Cha, H.J., Lee, C.B., Kim, B.S., Choi, M.S., Ruttenberg, K.C., 2005. Early diagenetic redistribution and burial of phosphorus in the sediments of the southwestern East Sea (Japan Sea). Mar. Geol. 216, 127–143.
Chen, C.T.A., 2009. Chemical and physical fronts in the Bohai, Yellow and East China seas. J. Mar. Syst. 78, 394–410.
Egger, M., Jilbert, T., Behrends, T., Rivard, C., Slomp, C.P., 2015. Vivianite is a major sink for phosphorus in methanogenic coastal surface sediments. Geochim. Cosmochim. Acta 217–235.
Fang, T.H., Chen, J.L., Huh, C.A., 2007. Sedimentary phosphorus species and sedimentation flux in the East China Sea. Cont. Shelf Res. 27, 1465–1476.
Gao, C.M., Zhu, Z., Wang, G.Q., Zhang, S., 2015. The distribution of phosphorus forms and its environmental significance in the marine ranching demonstration area of Haizhou Bay sediment. China Environ. Sci. 35, 3437–3444.
Gao, T.C., 2019. Exchange Fluxes of Nutrients Across Sediment-water Interface in the Muping Marine Ranch and Its Adjacent Waters. M.S. Thesis. University of Chinese Academy of Sciences, Beijing, China (97p).
Gu, S., Petitjean, P., Li, Q., Pinay, G., 2019. Respective roles of Fe-oxyhydroxide dissolution, pH changes and sediment inputs in dissolved phosphorus release from wetland soils under anoxic conditions. Geoderma 338, 365–374.
He, T., Xie, J., Yu, H., Fanf, H., 2010. Distribution characteristics of phosphorus forms in surface sediments in the Daya Bay. Acta Sci. Nat. Univ. Sunyatseni 49, 126–131.
Hou, L.J., Liu, M., Yang, Y., Ou, D.N., Lin, X., Chen, H., Xu, S.Y., 2009. Phosphorus speciation and availability in intertidal sediments of the Yangtze Estuary, China. Appl. Geochem. 24, 120–128.
Ingall, E., Jahnke, R., 1994. Evidence for enhanced phosphorus regeneration from marine sediments overlain by oxygen depleted waters. Geochim. Cosmochim. Acta 58, 2571–2575.
Kang, X.M., Song, J.M., Yuan, H.M., Yuan, H.M., Shi, X., Yang, W.F., Li, X.G., Li, N., Duan, L.Q., 2017. Phosphorus speciation and its bioavailability in sediments of the Jiaozhou Bay. Estuar. Coast. Shelf Sci. 188, 127–136.
Kraal, P., Slomp, C.P., Reed, D.C., Reichart, G.J., Poulton, S.W., 2012. Sedimentary phosphorus and iron cycling in and below the oxygen minimum zone of the northern Arabian Sea. Biogeosciences 9, 2603–2624.
Lin, P., Klump, J.V., Guo, L., 2016. Dynamics of dissolved and particulate phosphorus influenced by seasonal hypoxia in Green Bay, Lake Michigan. Sci. Total Environ. 541, 1070–1082.
Liu, S.M., Qi, X.H., Li, X.N., Ye, H.R., Wu, Y., Ren, J.L., Zhang, J., Xu, W.Y., 2016b. Nutrient dynamics from the Changjiang (Yangtze River) estuary to the East China Sea. J. Mar. Syst. 154, 15–27.
Liu, J., Song, J., Yuan, H., Li, X., Li, N., Duan, L., 2019. Biogenic matter characteristics, deposition flux correction, and internal phosphorus transformation in Jiaozhou Bay, North China. J. Mar. Syst. 196, 1–13.
Liu, J., Krom, M.D., Ran, X., Zang, J., Liu, J., Yao, Q., Yu, Z., 2020. Sedimentary phosphorus cycling and budget in the seasonally hypoxic coastal area of Changjiang Estuary. Sci. Total Environ. 713, 136389.
Liu, J., Zang, J., Zhao, C., Yu, Z., Xu, B., Li, J., Ran, X., 2016a. Phosphorus speciation, transformation, and preservation in the coastal area of Rushan Bay. Sci. Total Environ. 565, 258–270.
Liu, S.M., Zhang, J., Li, D., 2004. Phosphorus cycling in sediments of the Bohai and Yellow Seas. Estuar. Coast. Shelf Sci. 59, 209–218.
März, C., Poulton, S.W., Wagner, T., Schnetger, B., Brumsack, H.J., 2014. Phosphorus burial and diagenesis in the central Bering Sea (Bowers Ridge, IODP Site U1341): perspectives on the marine P cycle. Chem. Geol. 363, 270–282.
Meng, J., Yao, Q.Z., Chen, H.T., Yu, Z.G., 2012. Forms and distributions of particulate phosphorus in the surface sediments of North Yellow Sea. Environ. Sci. 33, 3361–3367.
Meng, J., Yao, P., Yu, Z., Bianchi, T.S., Zhao, B., Pan, H., Li, D., 2014. Speciation, bioavailability and preservation of phosphorus in surface sediments of the Changjiang Estuary and adjacent East China Sea inner shelf. Estuar. Coast. Shelf Sci. 144, 27–38.
Meng, J., Yao, P., Bianchi, T.S., Li, D., Zhao, B., Xu, B., Yu, Z., 2015. Detrital phosphorus as a proxy of flooding events in the Changjiang River Basin. Sci. Total Environ. 517, 22–30.
Monbet, P., Brunskill, G.J., Zagorskis, I., Pfitzner, J., 2007. Phosphorus speciation in the sediment and mass balance for the central region of the Great Barrier Reef continental shelf (Australia). Geochim. Cosmochim. Acta 71, 2762–2779.
Mort, H.P., Slomp, C.P., Gustafsson, B.G., Andersen, T.J., 2010. Phosphorus recycling and burial in Baltic Sea sediments with contrasting redox conditions. Geochim. Cosmochim. Acta 74, 1350–1362.
Mudroch, A., Azcue, J.M., 1995. Manual of Aquatic Sediment Sampling. Lewis Publishers, pp. 194–200.
Niu, Y.L., 2014. Seasonal Variation in Carbon, Nitrogen, Phosphorus and Silicon Budgets of Filter-feeding Shellfish in Sanggou Bay. M.S. Thesis. Zhejiang Ocean University, China (79p).
Pan, F., Guo, Z., Cai, Y., Fu, Y., Wu, J., Wang, B., Gao, A., 2020. Cyclical patterns and (im)mobilization mechanisms of phosphorus in sediments from a small creek estuary:

evidence from in situ monthly sampling and indoor experiments. Water Res. 171, 115479.
Picard, A., Gartman, A., Cosmidis, J., Obst, M., Girguis, P.R., 2019. Authigenic metastable iron sulfide minerals preserve microbial organic carbon in anoxic environments. Chem. Geol. 530, 119343.
Prasad, M.B.K., Ramanathan, A.L., 2010. Characterization of phosphorus fractions in the sediments of a tropical intertidal mangrove ecosystem. Wetl. Ecol. Manag. 18, 165–175.
Programme, U.N.E., Rantala, R.T.T., 1992. Manual for the geochemical analyses of marine sediments and suspended particulate matter. Earth Sci. Rev. 32, 235–283.
Qi, J., Li, F.Y., Song, J.M., Gao, S., Wang, G.Z., 2004. Sedimentation rate and flux of the North Yellow Sea. Mar. Geol. Quat. Geol. 24 (2), 9–13.
Qi, X., Liu, S., Zhang, J., Ren, J., Zhang, G., 2011. Cycling of phosphorus in the Jiaozhou Bay. Acta Oceanol. Sin. 30 (2), 62–74.
Redfield, A.C., 1963. The influence of organisms on the composition of seawater. The Sea. Wiley Interscience, New York, pp. 26–77.
Rucinski, D.K., DePinto, J.V., Beletsky, D., Scavia, D., 2016. Modeling hypoxia in the central basin of Lake Erie under potential phosphorus load reduction scenarios. J. Great Lakes Res. 42, 1206–1211.
Ruttenberg, K.C., 1992. Development of a sequential extraction method for different forms of phosphorus in marine sediments. Limnol. Oceanogr. 37, 1460–1482.
Ruttenberg, K.C., Berner, R.A., 1993. Authigenic apatite formation and burial in sediments from non-upwelling, continental margin environments. Geochim. Cosmochim. Acta 57, 991–1007.
Rydin, E., Malmaeus, J.M., Karlsson, O.M., Jonsson, P., 2011. Phosphorus release from coastal Baltic Sea sediments as estimated from sediment profiles. Estuar. Coast. Shelf Sci. 92, 111–117.
Song, J.M., 2010. Biogeochemical Processes of Biogenic Elements in China Marginal Seas. Springer, Berlin Heidelberg (676p).
Van der Zee, C., Slomp, C.P., van Raaphorst, W., 2002. Authigenic P formation and reactive P burial in sediments of the Nazaré canyon on the Iberian margin (NE Atlantic). Chem. Ecol. 185, 379–392.
Viktorsson, L., Almroth-Rosell, E., Tengberg, A., Vankevich, R., Neelov, I., Isaev, A., Hall, P.O., 2012. Benthic phosphorus dynamics in the Gulf of Finland, Baltic Sea. Aquat. Geochem. 18, 543–564.
Wang, Y., Liu, D., Richard, P., Li, X., 2013. A geochemical record of environmental changes in sediments from Sishili Bay, northern Yellow Sea, China: anthropogenic influence on organic matter sources and composition over the last 100 years. Mar. Pollut. Bull. 77, 227–236.
Yang, B., Gao, X., 2019. Chromophoric dissolved organic matter in summer in a coastal mariculture region of northern Shandong Peninsula, North Yellow Sea. Cont. Shelf Res. 176, 19–35.
Yang, B., Song, G.D., Liu, S.M., Jin, J., 2017. Phosphorus recycling and burial in core sediments of the East China Sea. Mar. Chem. 192, 59–72.
Yang, B., Gao, X., Xing, Q., 2018. Geochemistry of organic carbon in surface sediments of a summer hypoxic region in the coastal waters of northern Shandong Peninsula. Cont. Shelf Res. 171, 113–125.
Yang, B., Lan, R.Z., Lu, D.L., Dan, S.F., Kang, Z.J., Jiang, Q.C., Zhong, Q.P., 2019. Phosphorus biogeochemical cycling in intertidal surface sediments from the Maowei Sea in the northern Beibu Gulf. Reg. Stud. Mar. Sci. 28, 100624.
Yang, B., Gao, X., Zhao, J., Lu, Y., Gao, T., 2020a. Biogeochemistry of dissolved inorganic nutrients in an oligotrophic coastal mariculture region of the northern Shandong Peninsula, north Yellow Sea. Mar. Pollut. Bull. 150, 110693.
Yang, C., Yang, P., Geng, J., Yin, H., Chen, K., 2020b. Sediment internal nutrient loading in the most polluted area of a shallow eutrophic lake (Lake Chaohu, China) and its contribution to lake eutrophication. Environ. Pollut. 262, 114292.
Zhang, L., Wang, L., Yin, K.D., Lü, Y., Zhang, D.R., Yang, Y.Q., Huang, X.P., 2013a. Pore water nutrient characteristics and the fluxes across the sediment in the Pearl River estuary and adjacent waters, China. Estuar. Coast. Shelf Sci. 133, 182–192.
Zhang, W., White, J.R., DeLaune, R.D., 2012. Diverted Mississippi River sediment as a potential phosphorus source affecting coastal Louisiana water quality. J. Freshw. Ecol. 27, 575–586.
Zhang, X.Y., Yang, Q., Sun, Y., Shi, X.Y., Jiang, S.L., 2013b. Forms and bioavailability of phosphorus in sediment cores of culture zones in Sanggou Bay. Prog. Fish. Sci. 34 (2), 36–44.
Zhang, X.Y., Yang, Q., Sun, Y., 2013c. The distribution of phosphorus forms and bioavailability in sediments from Huang Dong Hai continental shelf. Acta Ecol. Sin. 33, 3509–3519.
Zhang, Y., Gao, X., Guo, W., Zhao, J., Li, Y., 2018. Origin and dynamics of dissolved organic matter in a mariculture area suffering from summertime hypoxia and acidification. Front. Mar. Sci. 5, 325.
Zhao, Y., Zhang, J., Lin, F., Ren, J.S., Sun, K., Liu, Y., 2019. An ecosystem model for estimating shellfish production carrying capacity in bottom culture systems. Ecol. Model. 393, 1–11.
Zhou, F., Gao, X., Yuan, H., Song, J., Chen, C.T.A., Lui, H.K., Zhang, Y., 2016. Geochemical forms and seasonal variations of phosphorus in surface sediments of the East China Sea shelf. J. Mar. Syst. 159, 41–54.
Zhuang, W., Gao, X., Zhang, Y., Xing, Q., Tosi, L., Qin, S., 2014. Geochemical characteristics of phosphorus in surface sediments of two major Chinese mariculture areas: the Laizhou Bay and the coastal waters of the Zhangzi Island. Mar. Pollut. Bull. 83, 343–351.
Zilius, M., Giordani, G., Petkuviene, J., Lubiene, I., Ruginis, T., Bartoli, M., 2015. Phosphorus mobility under short-term anoxic conditions in two shallow eutrophic coastal systems (Curonian and Sacca di Goro lagoons). Estuar. Coast. Shelf Sci. 164, 134–146.